SCIENCE CHINA
Physics, Mechanics & Astronomy

• Research Paper •
Special Issue: Forward for the Department of Engineering Mechanics, Tsinghua University

April 2011 Vol.54 No.4: 792–802
doi: 10.1007/s11433-011-4289-x

Optimal four-impulse rendezvous between coplanar elliptical orbits

WANG JianXia[1], BAOYIN HeXi[1*], LI JunFeng[1] & SUN FuChun[2]

[1] *School of Aerospace, Tsinghua University, Beijing 100084, China;*
[2] *Department of Computer Science and Technology, Tsinghua University, Beijing 100084, China*

Received December 12, 2010; accepted January 27, 2011; published online February 24, 2011

Rendezvous in circular or near circular orbits has been investigated in great detail, while rendezvous in arbitrary eccentricity elliptical orbits is not sufficiently explored. Among the various optimization methods proposed for fuel optimal orbital rendezvous, Lawden's primer vector theory is favored by many researchers with its clear physical concept and simplicity in solution. Prussing has applied the primer vector optimization theory to minimum-fuel, multiple-impulse, time-fixed orbital rendezvous in a near circular orbit and achieved great success. Extending Prussing's work, this paper will employ the primer vector theory to study trajectory optimization problems of arbitrary eccentricity elliptical orbit rendezvous. Based on linearized equations of relative motion on elliptical reference orbit (referred to as T-H equations), the primer vector theory is used to deal with time-fixed multiple-impulse optimal rendezvous between two coplanar, coaxial elliptical orbits with arbitrary large eccentricity. A parameter adjustment method is developed for the prime vector to satisfy the Lawden's necessary condition for the optimal solution. Finally, the optimal multiple-impulse rendezvous solution including the time, direction and magnitudes of the impulse is obtained by solving the two-point boundary value problem. The rendezvous error of the linearized equation is also analyzed. The simulation results confirmed the analyzed results that the rendezvous error is small for the small eccentricity case and is large for the higher eccentricity. For better rendezvous accuracy of high eccentricity orbits, a combined method of multiplier penalty function with the simplex search method is used for local optimization. The simplex search method is sensitive to the initial values of optimization variables, but the simulation results show that initial values with the primer vector theory, and the local optimization algorithm can improve the rendezvous accuracy effectively with fast convergence, because the optimal results obtained by the primer vector theory are already very close to the actual optimal solution. If the initial values are taken randomly, it is difficult to converge to the optimal solution.

elliptical orbit rendezvous, primer vector, fuel optimal

PACS: 95.10.Eg, 45.50.Pk

Nomenclature

x,z chaser relative state vector in the target orbital coordinate frame
ω orbital rate of target
h orbital angular momentum of target orbit
$k=\sqrt{h/p^2}$ constant
θ true anomaly
e eccentricity of target orbit
$\rho=1+e\cos\theta$
$c=\rho\cos\theta$
$s=\rho\sin\theta$
$\boldsymbol{p}$ primer vector
λ transverse component of primer vector
υ radial component of primer vector
$\boldsymbol{R}$ vector from the center of gravity to the target

*Corresponding author (email: baoyin@tsinghua.edu.cn)

spacecraft
- $\boldsymbol{r}$ vector from the target spacecraft to the chaser spacecraft
- $\boldsymbol{v}$ velocity vector from the target spacecraft to the chaser spacecraft
- t time
- μ gravity constant
- $J = k^2(t - t_0)$
- M mean anomaly
- $\bar{\omega}$ mean angular velocity
- Δ a change in the variable which it precedes
- a semi-major axis of target orbit
- p semi-latus rectum of target orbit
- β initial phase between the chaser spacecraft and the target spacecraft

Subscripts

- 0 initial value
- F final value
- C chaser spacecraft
- T target spacecraft
- ref reference point

1 Introduction

The primer vector theory is first proposed by Lawden [1], applicable in flight trajectory optimization, and has been widely used in space rendezvous optimization. Lion and Handelsman [2] developed the primer vector theory to determine how a given non-optimal trajectory can be improved by additional impulse and initial or/and final coasts. Jezewski and Rozendaal [3] presented a multi-impulse algorithm to orbital targeting problems based on Lion and Handelsman. Prussing [4–6] used the primer vector theory to investigate minimum-fuel, multiple-impulse and fixed-time orbital rendezvous in the vicinity of a circular orbit, and obtained some new results. Frank and Plexico [7] proposed mean velocity reference orbit for rendezvous in a circular orbit, which is more accurate than the mean radius reference orbit of Prussing in describing the impulse locations and magnitudes. Carter [8,9] presented an algorithm based on the quadratic formula for calculating four-impulse solutions, which is suitable for the optimal impulse rendezvous problem in the vicinity of a circular orbit. Prussing [10] demonstrated that Lawden's necessary conditions are also sufficient conditions for an optimal impulsive transfer in the linearized system, and proved that for linearized equations of motion, n impulses at most are needed for optimization in the n-dimensional state space. Necessary and sufficient conditions for optimal impulse rendezvous problems are obtained without utilizing specialized results from the optimization theory and control theory by Carter [11], which applied in a circular orbit rendezvous, and solutions of a specific set of equations are reduced from solving the two-point boundary-value problem.

For elliptical orbit rendezvous, people proposed relative motion on an elliptical orbit. The outstanding representative among them is Lawden's equation [12], in which an analytical solution can be obtained. A similar solution is also got by Hempel and Tschauner [13] for an elliptical reference orbit. Yamanaka and Ankersen [14] obtained a new and simpler solution to differential equations of relative motion on an arbitrary elliptical orbit, which is useful for engineering application. Lawden [15,16] achieved lots of useful results in optimal transfer between coplanar elliptical orbits. Based on his work, Carter [17] further obtained the solution to the problem of impulsive minimal solution subject to linear equations of motion, and applied this work to planar rendezvous problems in Keplerian orbit using the Tschauner-Hempel equations with a special emphasis on four-impulse solutions, and degenerate five-impulse solutions were found for higher eccentricity elliptical orbits.

In recent years, evolutionary optimization algorithms, such as genetic algorithms (GA), are widely used in optimal rendezvous. Kim el al. [18] investigated two-impulse minimum-fuel rendezvous using GA. However, it is difficult to find the genetic parameters and weighing factors of the fitness function converging to the global optimal solution.

This paper will apply the primer vector theory and extend Prussing's work to elliptical orbit to deal with the fuel- optimal, four-impulse elliptical orbit rendezvous. Based on Tschauner-Hempel's linearized equations of relative motion on an elliptical reference orbit, the primer vector theory is used to study time-fixed multiple-impulse optimal rendezvous between two coplanar, coaxial elliptical orbits with the similar eccentricities. A parameter adjustment method is developed to make the prime vector satisfy the Lawden's necessary condition for the optimal solution, and the optimal multiple-impulse rendezvous solution including the time and direction is obtained. Finally, the magnitudes of impulse are obtained by solving the two-point boundary value problem. The rendezvous error is analyzed also. The simulation results show that the rendezvous error is small for small eccentricity cases and is larger for higher eccentricity cases. Therefore, combination of multiplier penalty function with the simplex search method is applied for high eccentricity elliptical orbit rendezvous to improve the rendezvous accuracy.

2 Linearized equations of motion and the primer vector

2.1 Linearized equations of motion on an elliptical orbit

For rendezvous in elliptical orbits, the equations of prox-

imity relative motion in an arbitrary eccentricity elliptical target-orbit coordinate system are usually employed written as [14]

$$\ddot{x} = -k\omega^{3/2}x + 2\omega\dot{z} + \dot{\omega}z + \omega^2 x, \tag{1}$$

$$\ddot{z} = 2k\omega^{3/2}z - 2\omega\dot{x} - \dot{\omega}x + \omega^2 z, \tag{2}$$

where x, z are the transverse, radial components as coordinates illustrated in Figure 1. The prime denotes differentiation with respect to time t.

For the sake of a simpler expression of the relative motion, true anomaly θ of the target spacecraft is adopted as an independent variable instead of time t, and the transformation

$$\begin{bmatrix} \tilde{x} \\ \tilde{z} \end{bmatrix} = \rho \begin{bmatrix} x \\ z \end{bmatrix} \tag{3}$$

is also used, where $\rho = (1 + e\cos\theta)$, and e is the eccentricity of the target spacecraft orbit. Consequently, the equations of relative motion become rather simpler in dimensionless form [14]

$$\tilde{x}'' = 2\tilde{z}', \tag{4}$$

$$\tilde{z}'' = 3\tilde{z}/\rho - 2\tilde{x}', \tag{5}$$

where the prime denotes differentiation with respect to the true anomaly θ. Then, the in-plane state transition matrix of eqs. (4) and (5) can be obtained as [14]

$$\boldsymbol{\Phi}(\theta, \theta_0) = \boldsymbol{\Phi}_\theta \boldsymbol{\Phi}_{\theta_0}^{-1}, \tag{6}$$

where $\boldsymbol{\Phi}_{\theta 0}$ is the in-plane fundamental matrix solution associated with eqs. (4) and (5) having an expression as

$$\boldsymbol{\Phi}_{\theta 0} = \begin{bmatrix} 1 & -c(1+1/\rho) & s(1+1/\rho) & 0 \\ 0 & s & c & 2 \\ 0 & 2s & 2c-e & 3 \\ 0 & s' & c' & -3es/\rho^2 \end{bmatrix}, \tag{7}$$

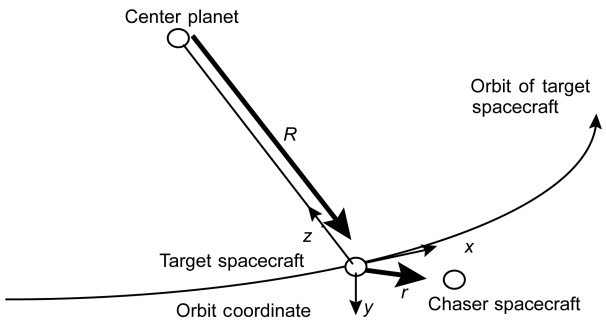

Figure 1 Coordinates definition.

where $s = \rho\sin\theta$, $c = \rho\cos\theta$, $s' = \cos\theta + e\cos 2\theta$, $c' = -(\sin\theta + e\sin 2\theta)$.

2.2 Necessary conditions for an optimal impulsive transfer

The necessary conditions for an optimal impulsive orbit transfer are expressed conveniently in terms of the primer vector, the vector of adjoint variables associated with the vehicle velocity vector. From the definition of the adjoint equations and the fact that the gravity gradient matrix is symmetric, one can show that the primer vector $\boldsymbol{p}$ satisfies the same differential equation as the first-order variation in the position vector $\delta\boldsymbol{r}$, namely,

$$\ddot{\boldsymbol{p}} = \boldsymbol{G}(\boldsymbol{r})\boldsymbol{p}, \tag{8}$$

where $\boldsymbol{G}(\boldsymbol{r})$ is the gravity gradient matrix evaluated along a reference solution to the orbit equations. The primer vector $\boldsymbol{p}$ has transverse, radial, and normal components, (λ, υ, w), respectively. On an elliptical orbit, eq. (8) is reduced to an identical form as eqs. (4) and (5). Hence, the primer vector solution for the in-plane components can be written as

$$\lambda = A(\rho+1)\sin(\theta+\psi) + 3B\rho^2 J + C, \tag{9}$$

$$\upsilon = A\rho\cos(\theta+\psi) - 3Be\rho J\sin\theta + 2B. \tag{10}$$

For the solutions to eqs. (4)–(5), please see Appendix. where A, B, C, ψ are constant, $J = k^2(t - t_0)$, $k = \mu/h^{3/2}$ = const, and t_0 represents initial time, μ is gravity constant, h is orbital angular momentum of the target spacecraft. The arbitrary constants A, B, C and ψ must be determined such that Lawden's necessary conditions are satisfied. The necessary conditions for an optimal impulsive transfer first are obtained by Lawden [1] and its application is introduced by Carter [9,11].

(1) The primer vector and its first time derivative must be continuous everywhere;

(2) the thrust impulses must be applied in the direction of the primer vector at the times for which the magnitude p of the primer vector is unity;

(3) the magnitude of the primer must not exceed unity during the transfer ($p \leqslant 1$);

(4) as a consequence of these conditions, at impulse times which are not the initial or final time, $\dot{p} = 0$.

For $t_0 = 0$, $\theta_0 = \dfrac{\pi}{12}$, a typical time history of a primer vector and its magnitude for an optimal four-impulse transfer are shown in Figure 2, where A=0.3613, B=0.08, C= 0.0383.

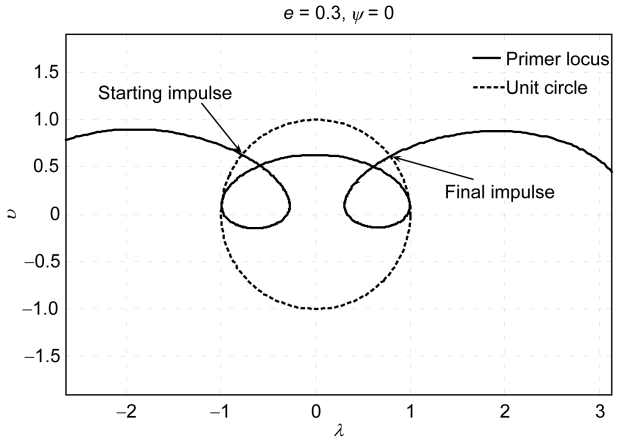

Figure 2 Primer locus diagram for a four-impulse optimal transfer.

3 Four-impulse primer vector solutions

3.1 Primer vector and its locus

The arbitrary constants in eqs. (9) and (10) characterize the locus of primer vector as follows: A determines scale of the plot, B characterizes shape of the locus, and C positions the locus along the λ axis. The details are summarized in Table 1. For a planar problem, solutions to the primer vector equation which satisfies the necessary conditions for an optimal transfer can be constructed geometrically using the primer locus diagram. For a specified fixed non-dimensional transfer time $t_F - t_0$, the necessary conditions require the locus to be smooth and lie on or inside a unit circle centered at the origin of the $\lambda - \upsilon$ plane ($p \leqslant 1$ for all $t \in [t_0, t_F]$), and that the locus is tangent to the unit circle($\dot{p} = 0$) for midterm impulses. The optimum times to apply the impulses are those times for which the locus intersects the unit circle ($p = 1$); the thrust directions are given by the λ and υ components at these moments [1].

The parameters' influence on the locus shape is also shown in Figure 3.

3.2 Construction of primer vector solutions

According to the abovementioned property, the primer vector must satisfy the following equations for the four-impulse optimal transfer

$$\lambda^2(t_i) + \upsilon^2(t_i) = 1 \quad (i = 1,2,3,4), \tag{11}$$

$$\lambda(t_j)\dot{\lambda}(t_j) + \upsilon(t_j)\dot{\upsilon}(t_j) = 0 \quad (j = 2,3). \tag{12}$$

Here, eqs. (11) and (12) present six quadratic equations with six unknowns to determine the primer vector $\boldsymbol{p}$. These equations generally can't be solved analytically. So other routes have to be found to solve them for our interested cases. A simple method is presented below by geometrical construction.

If the four parameters A, B, C, ψ are determined, then the primer locus is decided uniquely. According to the summary in Table 1, the influences of B, ψ on the locus are relatively complicated. If B, ψ are fixed firstly, then the locus is tangent to the unit circle by adjusting A, C. The process can be done as follows:

(1) Give arbitrary constants to A, C, and plot the locus diagram as Figure 4.

(2) To find two points on the locus, which are peak values near the zero, like F and G in Figure 4, calculate the difference between the primer value at these points and 1, representing them as c, d shown in Figure 4.

$$c = p(t_F) - 1, \tag{13}$$

$$d = p(t_G) - 1. \tag{14}$$

(3) Define

$$f = (c - d)/2. \tag{15}$$

In Figure 4 $f > 0$, so adjust C to have $f = 0$; and adjust A simultaneously to have $c = 0$. The adjusting steps are taken as

$$\Delta A = -c \cdot Kp_A, \tag{16}$$

Table 1 The parameters' influence on the locus shape

Parameters change	The shape and position of the primer locus change
Increase A	The loop is expanded and the position of the locus is unchanged.
Decrease A	The loop shrinks and the position of the locus is unchanged.
Increase B	The loop shrinks, the distance between two loops increases.
Decrease B	The loop is expanded, and the distance between two loops decreases.
Increase C	The shape is unchanged, and the position of the locus moves toward right.
Decrease C	The shape is unchanged, and the position of the locus moves toward left.
Increase ψ	The left loop shrinks, the right loop is expanded, the difference of two loops in size becomes large, and the position of the locus is unchanged.
Decrease ψ	The left loop is expanded, the right loop shrinks, the difference of two loops in size becomes large, and the position of the locus is unchanged.

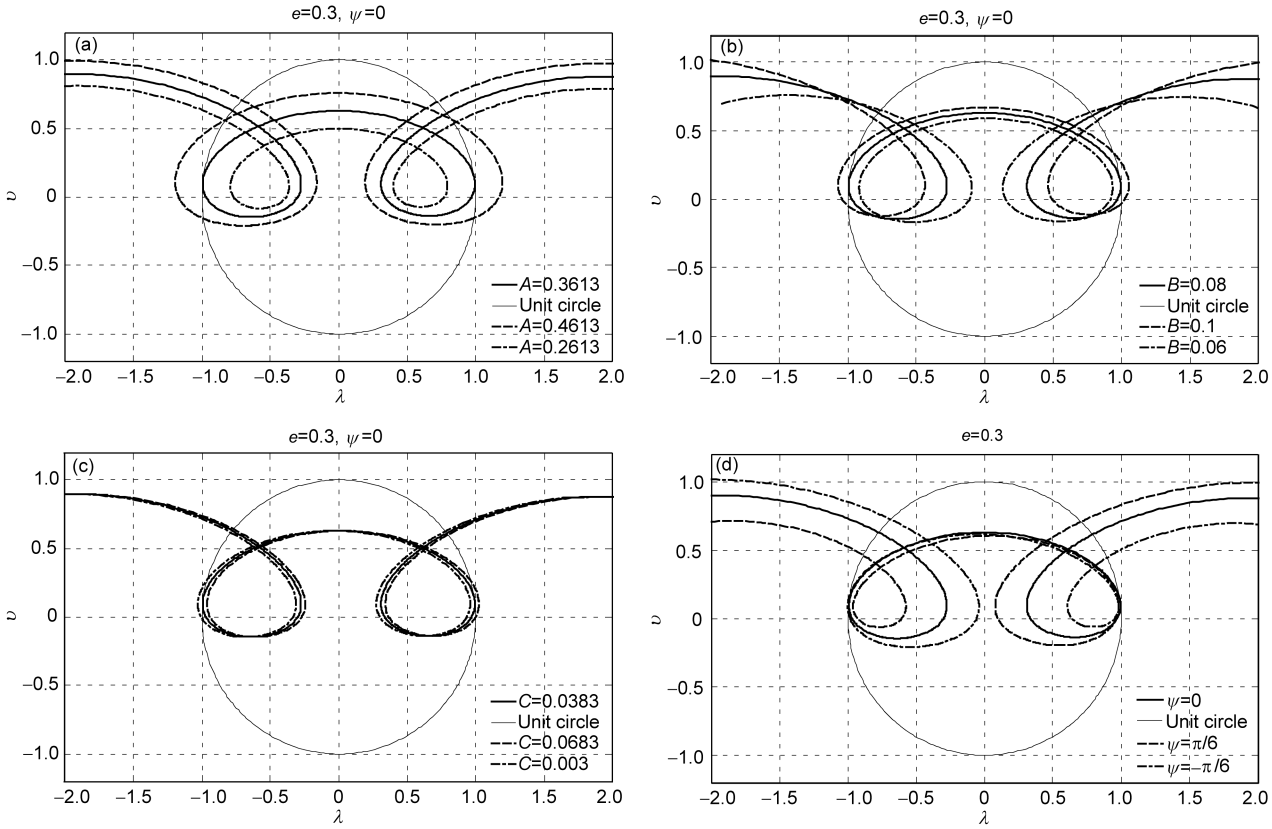

Figure 3 The parameters' influence on the locus shape. (a) B=0.08, C= 0.0383; (b) A=0.3613, C= 0.0383; (c) A=0.3613, B=0.08; (d) A=0.3613, B=0.08, C= 0.0383.

$$\Delta C = f \cdot Kp_{\mathrm{C}}, \tag{17}$$

where Kp_{A} and Kp_{C} are the proportionality factor, which is the ratio of the error of primer magnitude to the iterative step of A or C. The values range from 0 to 1. In the present paper, it is set $Kp_{\mathrm{A}} = 0.6$, $Kp_{\mathrm{C}} = 0.7$. If

$$\begin{cases} c = 0, \\ f = 0, \end{cases} \tag{18}$$

is obtained, that means

$$\begin{cases} c = 0, \\ d = 0. \end{cases} \tag{19}$$

Eq. (19) shows that Lawden's necessary conditions are satisfied.

The technique applied to construct primer vector solutions which satisfy the necessary conditions involves taking a locus shape by picking a value of constant B, ψ. After solutions are constructed, these constants are varied respectively in order to investigate all locus shapes of interest. In addition, for $B > B_{\max}$, the locus has no loops, and therefore no four-impulse optimal solutions can be constructed since the necessary tangency of the locus with the unit circle for a mid-course impulse is not possible. And for fixed B, the process is the same as the aforementioned by changing ψ. For a given pair of B, ψ, the method of evaluating the other constants for the locus is considered. It should be noted that, although fixed-time solutions are obtained, it is the constant B and ψ that is initially specified and not the transfer time. The value of the transfer time can be obtained from the construction. In the present paper, for different B and ψ, corresponding transfer times are obtained by the aforementioned method and the data are saved as database. Because the primer locus is decided uniquely by four parameters A, B, C, ψ, which means that if an transfer time is known, the only set of parameters A, B, C, ψ is obtained. For a rendezvous problem, transfer time is always known, so the database can be used to get relevant parameters B, ψ corresponding to the transfer time, and A, C are also decided.

4 Boundary-value problem for rendezvous

4.1 Definition of a reference orbit

To linearize the chaser's motion around a reference orbit, we set a reference point and a reference orbit between the chaser and target orbits as shown in Figure 5. The phases of the chaser spacecraft and reference point are identical at

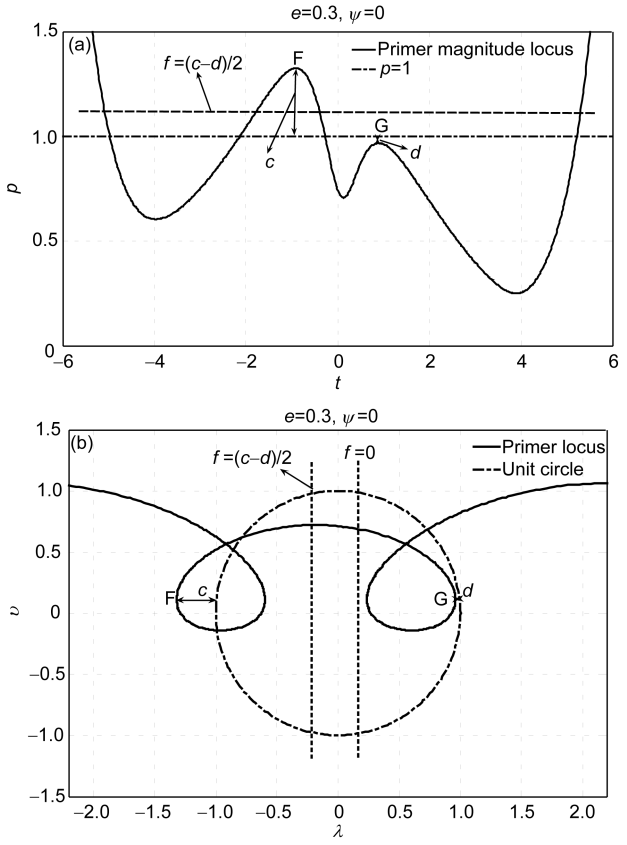

Figure 4 (a) Primer magnitude locus diagram for the four-impulse non-optimal transfer; (b) primer locus diagram for the four-impulse non-optimal transfer.

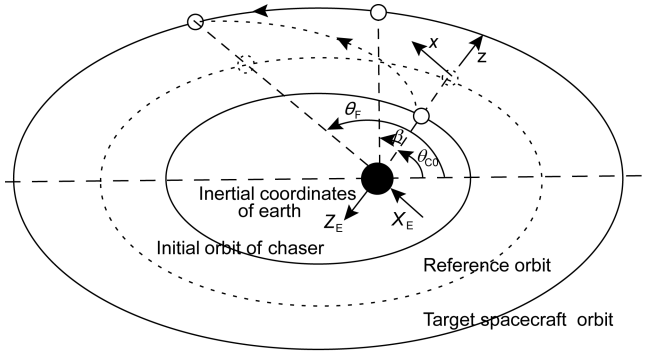

Figure 5 Elliptical reference orbit and coordinates definition.

both the initial and the arrival time, which indicates that the mean angular velocity of the chaser spacecraft is the same as the reference point during the rendezvous process. And the semimajor axis of the reference orbit is calculated by

$$M_{\mathrm{ref}} = M_{\mathrm{T}}, \tag{20}$$

$$\Delta M_{\mathrm{ref}} = M_{\mathrm{ref}} - M_{\mathrm{ref0}}, \tag{21}$$

$$\bar{\omega}_{\mathrm{ref}} = \Delta M_{\mathrm{ref}} / t_{\mathrm{F}}, \tag{22}$$

$$a_{\mathrm{ref}} = (\mu / \bar{\omega}_{\mathrm{ref}}^2)^{1/3}, \tag{23}$$

where M represents the mean anomaly, $\bar{\omega}$, mean angular velocity, the subscript 'ref' means the reference point, 'T' is the target spacecraft, '0' presents initial value, and 'F' means final value.

4.2 Rendezvous boundary-value problem

This paper assumes that the chaser's initial orbit and the target spacecraft orbit are coplanar, coaxial ellipses, which have the same eccentricity. For a coplanar rendezvous problem, the state variation of the chaser spacecraft with regard to the reference point is shown as follows:

$$\delta \boldsymbol{x} = \begin{pmatrix} \delta \boldsymbol{r} \\ \delta \boldsymbol{v} \end{pmatrix}, \tag{24}$$

where the position variation $\delta \boldsymbol{r}$ and the velocity variation $\delta \boldsymbol{v}$ both have two components. Then using the linearized relative equation, the boundary-value equation can be obtained as [4]

$$\delta \boldsymbol{x}_{\mathrm{F}} = \boldsymbol{\Phi}_{\mathrm{F0}} \delta \boldsymbol{x}_0 + \boldsymbol{W}(t_j, \boldsymbol{u}_j) \Delta \boldsymbol{V}, \tag{25}$$

where $\delta \boldsymbol{x}_0$ denotes the state variation of the chaser spacecraft at the initial time, $t_0 = 0$; $\delta \boldsymbol{x}_{\mathrm{F}}$ denotes the final state variation, which for rendezvous is the state variation of the target with respect to the reference point at the final time. $\boldsymbol{\Phi}_{\mathrm{F0}}$ is the state transition matrix of the linear system; $\Delta \boldsymbol{V}$ is a vector composed of the magnitudes of n impulses [4]. For a fixed-time rendezvous the initial state variation and the anticipant terminal state variation are known. And matrix $\boldsymbol{W}$ is obtained from the geometrical construction of primer-locus. The boundary-value problem is then to solve $\Delta \boldsymbol{V}$, which will complete the optimal rendezvous.

In eqs. (11) and (12), the six quadratic equations suggest that the primer vector $\boldsymbol{p}$ may have $2^6 = 64$ solutions satisfying the necessary conditions for the same initial and terminal conditions. Each solution to the primer vector corresponds with the only one solution to $\Delta \boldsymbol{V}$, so the $\Delta \boldsymbol{V}$ has multi-solutions. However, not all solutions of $\Delta \boldsymbol{V}$ are admitted, since the impulse thrust direction is along with the primer vector direction. If $\Delta \boldsymbol{V}$ has some negative components, that implies the impulse and the primer vector direction are opposite. It is inadmissible due to violating one of Lawden's necessary conditions for optimal transfer although this solution satisfies the boundary conditions. So the conditions for an admissible solution are as follows [4]:

$$\Delta V_j \geqslant 0, \quad j = 1, 2, \cdots, n, \tag{26}$$

$$\min \sum_{j=1}^{n} \Delta V_j. \tag{27}$$

Usually, only one solution satisfies eq. (26) in theory. In some special situations, there are more than one solution in

that condition. Non-optimal solutions are eliminated by testing $\sum_{j=1}^{n}\Delta V_j$ which is a minimum [11].

5 Rendezvous error analysis

Just how many errors will be brought into the linearized equation for larger eccentricity orbits? Here the linearized rendezvous error is analyzed.

5.1 Position error generated by secular terms

The solution to linearized equations of in-plane relative motion can be obtained as [14]

$$\tilde{x} = K_1 - K_2 c(1+1/\rho) + K_3 s(1+1/\rho) + 3K_4\rho^2 J, \quad (28)$$

$$\tilde{z} = K_2 s + K_3 c + K_4(2-3esJ), \quad (29)$$

where K_1, K_2, K_3, K_4 are arbitrary constants. For a linearized model, an error is induced by linearization and the secular term of transverse and radial is respectively

$$\tilde{x}: \quad 3K_4\rho^2 J = -3K_{z2}e\rho^2 J, \quad (30)$$

$$\tilde{z}: \quad -3K_4 e\rho J\sin\theta = 3K_{z2}e^2\rho J\sin\theta, \quad (31)$$

where $k^2 = \dfrac{\mu^2}{h^3} = \sqrt{\mu}p^{-1.5}$, $J = k^2(t-t_0)$, and K_{z2} is an integral constant [14].

Herein the following type of Taylor series is applied to error analysis

$$(1+x)^m = 1 + mx + \frac{m(m-1)}{2!}x^2 + \cdots + \frac{m(m-1)\cdots(m-n+1)}{n!}x^n + o(x^{n+1}). \quad (-1<x<1) \quad (32)$$

Applying eq. (32), $p^{-1.5} = (1-e^2)^{-1.5}$ (dimensionless $a=1$) becomes

$$(1-e^2)^{-1.5} = 1 + 1.5e^2 + 1.875e^4 + 2.1875e^6 + \cdots \approx 1 + 1.5e^2. \quad (33)$$

Substituting eq. (33) into eqs. (30)–(31) yields the secular term of transverse

$$\begin{aligned} -3K_{z2}e\rho^2 J &\approx -3K_{z2}e\rho^2\sqrt{\mu}(1+1.5e^2)(t-t_0) \\ &\leqslant 3\left|K_{z2}\right|e\rho^2\sqrt{\mu}(1+1.5e^2)(t-t_0) \\ &= 3\left|K_{z2}\right|e(1+e\cos\theta)^2\sqrt{\mu}(1+1.5e^2)(t-t_0) \\ &\leqslant 3\left|K_{z2}\right|e(1+e)^2\sqrt{\mu}(1+1.5e^2)(t-t_0) \\ &= 3\left|K_{z2}\right|\sqrt{\mu}(e+2e^2+2.5e^3+3e^4+1.5e^5)(t-t_0). \end{aligned} \quad (34)$$

The secular term of radial is

$$\begin{aligned} 3K_{z2}e^2\rho J\sin\theta &\approx 3K_{z2}e^2\rho\sqrt{\mu}(1+1.5e^2)(t-t_0)\sin\theta \\ &\leqslant 3\left|K_{z2}\right|e^2\rho\sqrt{\mu}(1+1.5e^2)(t-t_0) \\ &= 3\left|K_{z2}\right|e^2(1+e\cos\theta)\sqrt{\mu}(1+1.5e^2)(t-t_0) \\ &\leqslant 3\left|K_{z2}\right|e^2(1+e)\sqrt{\mu}(1+1.5e^2)(t-t_0) \\ &= 3\left|K_{z2}\right|\sqrt{\mu}(e^2+e^3+1.5e^4+1.5e^5)(t-t_0). \end{aligned} \quad (35)$$

Eliminating the higher-order terms, eqs. (34) and (35) can now be expressed as

$$\tilde{x} \propto e(t-t_0), \quad (36)$$

$$\tilde{z} \propto e^2(t-t_0). \quad (37)$$

From eqs. (36) and (37), it can be found that the secular term is associated with eccentricity and rendezvous time. The effects of rendezvous by secular terms are shown in Table 2.

In Table 2, the rendezvous are two reference orbit periods, 4π. K_{z2} is calculated approximately from initial condition $\delta\boldsymbol{x}_0$. And errors in the Table 2 are the upper bound for corresponding eccentricity, because flight free is used to replace the impulse maneuver process, in which the value of the initial condition becomes larger than the impulse

Table 2 The rendezvous error generated by the secular terms

e	$\tilde{x}: 3\left\|K_{z2}\right\|e(t-t_0)$	Order of magnitude of $\tilde{x}$	$\tilde{z}: 3\left\|K_{z2}\right\|e^2(t-t_0)$	Order of magnitude of $\tilde{z}$
0.01	0.0868		0.0009	1×10^{-4}
0.02	0.0798		0.0016	
0.03	0.0725	1×10^{-2}	0.0022	1×10^{-3}
0.05	0.0573		0.0029	
0.1	0.0131		0.0013	
0.3	0.2816	1×10^{-1}	0.0845	1×10^{-2}
0.5	0.9951		0.4975	1×10^{-1}
0.7	3.2962	1×10^{0}	2.3073	1×10^{0}
0.9	22.8087	1×10^{1}	20.5278	1×10^{1}

maneuver. Table 2 indicates that the higher eccentricity, the larger the rendezvous error.

5.2 Velocity error generated by secular terms

The equations for the velocity can be obtained by differentiation of eqs. (28) and (29) [14]

$$\tilde{v}_x = 2K_2 s + K_3(2c - e) + 3K_4(1 - 2esJ), \tag{38}$$

$$\tilde{v}_z = K_2 s' + K_3 c' - 3K_4 e(s'J + s/\rho^2). \tag{39}$$

The secular terms of transverse and radial of velocity can be obtained as

$$\tilde{v}_x : \quad 3K_4(-2esJ) = -6K_4 e\rho \sin\theta J, \tag{40}$$

$$\tilde{v}_z : \quad -3K_4 es'J = -3K_4 e(\cos\theta + e\cos 2\theta)J. \tag{41}$$

Considering eq. (30), it yields

$$\frac{\tilde{v}_x}{\tilde{x}} = \frac{-6K_4 e\rho \sin\theta J}{3K_4\rho^2 J} = \frac{-2e\sin\theta}{\rho} \tag{42}$$

and furthermore,

$$\left|\frac{\tilde{v}_x}{\tilde{x}}\right| = \frac{2e|\sin\theta|}{1 + e\cos\theta} \leqslant \frac{2e|\sin\theta|}{e|\cos\theta|} = 2|\tan\theta|. \tag{43}$$

From eq. (43), $\tilde{v}_x/\tilde{x}$ is not relevant to eccentricity e and the order of magnitudes of $\tilde{v}_x$ and $\tilde{x}$ is the same.

In a similar manner, $\tilde{v}_z/\tilde{z}$ is obtained as follows:

$$\begin{aligned}\frac{\tilde{v}_z}{\tilde{z}} &= \frac{-3K_4 e(\cos\theta + e\cos 2\theta)J}{-3K_4 e\rho J\sin\theta} \\ &= \frac{(\cos\theta + e\cos 2\theta)}{\rho\sin\theta} = \frac{(\cos\theta + e\cos 2\theta)}{\sin\theta + \frac{1}{2}e\sin 2\theta}\end{aligned} \tag{44}$$

and

$$\left|\frac{\tilde{v}_z}{\tilde{z}}\right| = \frac{|\cos\theta + e\cos 2\theta|}{\left|\sin\theta + \frac{1}{2}e\sin 2\theta\right|} \approx 2\cot 2\theta. \tag{45}$$

From eq. (45), $\tilde{v}_z/\tilde{z}$ is not relevant to eccentricity e, and the order of magnitudes of $\tilde{v}_z$ and $\tilde{z}$ is identical. This is because the velocity is derivative of the position with respect to true anomaly θ, so the proportion of velocity and position has nothing to do with eccentricity e, and the order of magnitudes of velocity and position is identical.

6 Simulation

6.1 Optimal results of the primer vector

Here an optimal four-impulse coplanar elliptical orbit rendezvous example is demonstrated. Simulation conditions are summarized in Table 3, and here assume other parameters as R_{Earth}=6400 km; a_{C}=0.995× a_{ref}; a_{T}=1.005× a_{ref}; t_0=0; θ_{C0}=0; $i = \pi/2$; $\Omega = 0$; $\omega = 0$. The optimal results are presented in Table 4, 't_{F}' represents dimensionless transfer time, and 'β' initial phase.

Note that the values given in Table 4 are in a non-dimensional way associated with eq. (3)'s transformation. From Table 4, it can be found that the linearized rendezvous error becomes larger in the large eccentricity cases although the optimal impulses can be solved from the primer vector theory. To resolve this problem requires a local optimization method to refine the terminal rendezvous error.

6.2 Local optimization

6.2.1 Elimination of errors generated by the secular terms

From the simulation of the previous section, the rendezvous errors are large for high-eccentricity orbits if only the primer vector solution is used. It is obviously induced by linearization of the relative motion equations. If the rendezvous errors are expected to become small, a local optimization is needed and one algorithm presented in this paper is combined with multiplier penalty function and the simplex search method, and the initial value of local optimization is given by the primer vector results.

6.2.2 Determination of optimization variables

If the time, directions and magnitudes of impulses are taken as optimization variables, the optimization variable would become excessive. To simplify the problem, the present study takes the impulses magnitudes as optimization variables. The initial values of impulses magnitudes are

Table 3 Simulation conditions

Reference orbit	Perigee height (km)	The semimajor axis (km)	The rendezvous time (s)	Initial phase (rad)
e=0.01	300	6767.7	9277.5	0.08
e=0.05	300	7052.6	11375	0.10
e=0.1	300	7444.4	11115	0.10
e=0.3	300	9571.4	12279	0.12
e=0.5	300	13400	19116	0.20
e=0.7	300	22333	36556	0.40

Table 4 Optimal results

Optimal results\ Initial conditions	e=0.01 β=0.08 t_F=10.5205	e=0.05 β=0.10 t_F=12.1257	e=0.1 β=0.10 t_F=10.9256	e=0.3 β=0.12 t_F=8.2791	e=0.5 β=0.2 t_F=7.7807	e=0.7 β=0.4 t_F=6.9152
ΔV_1	0.0012	–0.0007	–0.0017	–0.0046	–0.0106	–0.0224
ΔV_2	0.0011	0.0022	0.0020	–0.0012	–0.0018	–0.2225
ΔV_3	–0.0012	–0.0023	–0.0024	–0.0014	0.0004	–0.2154
ΔV_4	–0.0015	0.0006	–0.0007	–0.0072	–0.0113	–0.0132
$\sum_{i=1}^{4}\lvert\Delta V_i\rvert$	0.0051	0.0058	0.0069	0.0144	0.0242	0.4735
$\tilde{x}_{\text{Error}}$	0.0064	0.0151	0.0708	–0.0953	–0.2242	–0.6300
$\tilde{z}_{\text{Error}}$	-0.0027	0.0339	–0.0050	–0.1134	–0.1710	–0.1730
$\tilde{v}_{x\text{Error}}$	0.0035	–0.0346	0.0183	0.0977	0.1887	0.4918
$\tilde{v}_{z\text{Error}}$	0.0055	0.0157	0.0638	–0.0905	–0.1711	–0.5151

obtained from the primer vector theory. The details of the local optimization algorithm are presented in the following part.

Objective function is taken as

$$obj = \boldsymbol{\lambda}\cdot\boldsymbol{h}_{\text{f}} + \frac{c_t}{2}\left|\boldsymbol{h}_{\text{f}}\right|^2, \tag{46}$$

where $\boldsymbol{h}_{\text{f}}$=[$\tilde{x}_{\text{Error}}$, $\tilde{z}_{\text{Error}}$, $\tilde{v}_{x\text{Error}}$, $\tilde{v}_{z\text{Error}}$], $\boldsymbol{\lambda}$ is the weight coefficient, and c_t is the penalty factor. The optimization objective is to reduce error $\boldsymbol{h}_{\text{f}}$ to zero. The coefficient and factor are given as

$$\boldsymbol{\lambda} = 6\times10^{m}\times\begin{bmatrix}1 & 1 & 1 & 1\end{bmatrix}^{\text{T}}, \tag{47}$$

$$c_t = 5\times10^{2m}, \tag{48}$$

where m is a positive integer which matches the order of magnitude of expected rendezvous error. Namely, if you expect the error to be 10^{-m}, then the coefficient and factor assignment take the expression of eqs. (47) and (48).

Optimization variables,

$$\Delta V_i \quad (i = 1,2,\cdots n). \tag{49}$$

Here a local optimization simulation is demonstrated. Local optimization process is performed by *fminsearch*, a Matlab software package, and the local optimization results are presented in Table 5. In example 1 the parameters are taken as $e = 0.5$, and $\beta = 0.2$.

In Table 5, the local optimal results are good, and the error is within the requirement, order of 10^{-8}. When the very high-precision is required, an iterative optimization algorithm is proposed, based on local optimization. For example, the results of Case 2 of Table 5 can be taken as the initial value of iterative optimization, and set m further as 10, and repeat the process of local optimization. The iterative optimization results are presented in Table 6 which shows that the satisfactory results are obtained in the further optimization.

In example 2, the parameters are taken as $e = 0.7$, and $\beta = 0.4$. The local optimization results are presented (m=8) in Table 7. If the higher-precision is needed, the iterative optimization should be used as in the previous example.

Example 3 takes $e = 0.7$ and $\beta = 0.4$, and demonstrates the sensitivity to the initial value. Initial values of $\Delta V_i (i = 1,2,\cdots n)$, $\Delta \boldsymbol{V}_0$, for the local optimization are given

Table 5 Local optimization results

	Case 1 m=6	Case 2 m=8	Case 3 m=10
ΔV_1	0.0014134	0.001413348	0.0014133569
ΔV_2	–0.0046143	–0.004614372	–0.004614415
ΔV_3	–0.0062474	–0.006247725	–0.006247746
ΔV_4	–0.0023565	–0.002354807	–0.00235478
$\sum_{i=1}^{4}\lvert\Delta V_i\rvert$	0.014632	0.01463025	0.014630299
$\tilde{x}_{\text{Error}}$	-1.2209×10^{-6}	-1.2585×10^{-8}	-0.3420×10^{-8}
$\tilde{z}_{\text{Error}}$	-1.1905×10^{-6}	-1.1488×10^{-8}	-1.788×10^{-8}
$\tilde{v}_{x\text{Error}}$	-1.1639×10^{-6}	-1.0747×10^{-8}	-1.620×10^{-8}
$\tilde{v}_{z\text{Error}}$	-1.1939×10^{-6}	-1.1971×10^{-8}	4.956×10^{-8}

Table 6 Iterative optimization results

Case 4	ΔV_1	ΔV_2	ΔV_3	ΔV_4
	0.001413348	–0.004614372	–0.0062477278	–0.00235478979
$\sum_{i=1}^{4}\lvert\Delta V_i\rvert$	$\tilde{x}_{\text{Error}}$	$\tilde{z}_{\text{Error}}$	$\tilde{v}_{x\text{Error}}$	$\tilde{v}_{z\text{Error}}$
0.0146302377	-1.199×10^{-10}	-1.199×10^{-10}	-1.200×10^{-10}	-1.198×10^{-10}

Table 7 Local optimization results

Case 5	ΔV_1	ΔV_2	ΔV_3	ΔV_4
	0.001703	0.01693	0.01547	–0.0007627
$\sum_{i=1}^{4}\lvert\Delta V_i\rvert$	$\tilde{x}_{\text{Error}}$	$\tilde{z}_{\text{Error}}$	$\tilde{v}_{x\text{Error}}$	$\tilde{v}_{z\text{Error}}$
0.03487	-1.201×10^{-8}	-1.198×10^{-8}	-1.200×10^{-8}	-1.201×10^{-8}

arbitrarily in case 6, and set $m=8$, namely $\boldsymbol{\lambda}=6\times10^{8}\times\left[1\quad 1\quad 1\quad 1\right]^{\mathrm{T}}$, $c_t=5\times10^{16}$.

The results in Table 8 show that in case 6 optimal results do not meet the requirement. The initial value of case 7 is taken as the primer vector solution, and the local optimization results exactly meet the error requirement. This shows that the local optimization algorithm is sensitive to the initial value, and the primer vector theory can exactly provide the initial value which is in the neighborhood of local optimization.

7 Conclusions

Based on linearized equations of relative motion around an elliptical reference orbit, the primer vector optimization theory is used to study time-fixed multiple-impulse optimal rendezvous between two coplanar, coaxial elliptical orbits with the similar eccentricities. A parameter adjustment method is developed to solve the prime vector equation to satisfy Lawden's necessary condition for the optimal solution. The optimal multiple-impulse rendezvous solution including the time and direction is obtained. Then, the magnitudes of impulse are obtained by solving the two-point boundary value problem. The rendezvous error analysis and simulation show that the rendezvous error is small for the small eccentricity case and is large for the high eccentricity if no local optimization is involved. To improve the high eccentricity elliptical orbit terminal rendezvous accuracy, we combine the multiplier penalty function with the simplex search method. The simulation shows that the local optimization algorithm has successfully improved the rendezvous accuracy with fast convergence. The simplex search method is sensitive to the initial value of optimization variables. If the initial values are taken randomly, it is difficulty to converge to the optimal results; but taken from the primer vector optimization, it can always get a high accuracy and fast converging solution even in the high eccentricity case.

Appendix A

In Yamanaka's [14] paper([see eq. (71)]), for coplanar elliptical orbits, the solutions of relative motion on an arbitrary elliptical orbit in dimensionless form are

Table 8 The local optimization results of different $\Delta\boldsymbol{V}_0$

	Case 6 $\Delta\boldsymbol{V}_0$=[–0.1, –0.1, –0.1, –0.1]	Case 7 $\Delta\boldsymbol{V}_0$=[–0.01, –0.1, –0.1, –0.01]
ΔV_1	–0.1822	0.001703
ΔV_2	–0.01866	0.01693
ΔV_3	0.1702	0.01547
ΔV_4	–0.07075	–0.0007627
$\sum_{i=1}^{4}\lvert\Delta V_i\rvert$	0.4418	0.0349
$\tilde{x}_{\text{Error}}$	0.06467	-1.203×10^{-8}
$\tilde{z}_{\text{Error}}$	–0.09546	-1.199×10^{-8}
$\tilde{v}_{x\text{Error}}$	–0.006780	-1.197×10^{-8}
$\tilde{v}_{z\text{Error}}$	–0.05557	-1.202×10^{-8}

$$\begin{aligned}\tilde{x} &= K_1 - K_2(\rho+1)\cos\theta + K_3(\rho+1)\sin\theta + 3K_4\rho^2 J \\ &= K_1 + (K_3\sin\theta - K_2\cos\theta)(\rho+1) + 3K_4\rho^2 J \\ &= K_1 + (\rho+1)\frac{1}{\sqrt{K_2^2+K_3^2}}\sin(\theta+\psi) + 3K_4\rho^2 J, \end{aligned} \tag{a1}$$

$$\begin{aligned}\tilde{z} &= K_2\rho\sin\theta + K_3\rho\cos\theta + K_4(2-3e\rho J\sin\theta) \\ &= \rho(K_2\sin\theta + K_3\cos\theta) + K_4(2-3e\rho J\sin\theta) \\ &= \rho\frac{1}{\sqrt{K_2^2+K_3^2}}\cos(\theta+\psi) + K_4(2-3e\rho J\sin\theta) \\ &= \rho\frac{1}{\sqrt{K_2^2+K_3^2}}\cos(\theta+\psi) - 3K_4 e\rho J\sin\theta + 2K_4, \end{aligned} \tag{a2}$$

by

$$\begin{aligned}K_3\sin\theta - K_2\cos\theta &= \frac{1}{\sqrt{K_2^2+K_3^2}}\sin(\theta+\psi), \\ K_2\sin\theta + K_3\cos\theta &= \frac{1}{\sqrt{K_2^2+K_3^2}}\cos(\theta+\psi). \end{aligned} \tag{a3}$$

So the solutions become

$$\tilde{x} = A(\rho+1)\sin(\theta+\psi) + 3B\rho^2 J + C, \tag{a4}$$

$$\tilde{z} = A\rho\cos(\theta+\psi) - 3Be\rho J\sin\theta + 2B \tag{a5}$$

in which $A = \frac{1}{\sqrt{K_2^2+K_3^2}}$, $B = K_4$, $C = K_1$, $\tan\psi = -\frac{K_2}{K_3}$.

This research was supported by the National Natural Science Foundation of China (Grant Nos. 10832004 and 11072122).

1 Lawden D F. Optimal Trajectories for Space Navigation. London: Butterworths, 1963
2 Lion P M, Handelsman H M. Primer vector on fixed-time impulsive trajectories. AIAA J, 1968, 6(1): 127–132
3 Jezewski D J, Rozendaal H L. An efficient method for calculating optimal free-space N-impulse trajectories. AIAA J, 1968, 6(11): 2160–2165
4 Prussing J E. Optimal Multi-impulse Orbital Rendezvous. Dissertation for Doctoral Degree. Thesis. Massachusetts: Massachusetts Institute of Technology, 1963
5 Prusing J E. Optimal four-impulse fixed-time rendezvous in the vicinity of a circular orbit. AIAA J, 1969, 7(5): 928–935
6 Prussing J E. Optimal two-and three- impulse fixed-time rendezvous in the vicinity of a circular orbit. AIAA J, 1970, 8(7): 1221–1228
7 Frank C L, Plexico L D. Improved solution of optimal impulsive fixed-time rendezvous. J Spacecr Rockets, 1982, 19(6): 521–528
8 Carter T E, Alvarez S A. Four-impulse rendezvous near circular orbit. AIAA/AAS, Astrodynamics Specialist Conference and Exhibit. Boston, MA, 1998,
9 Carter T E, Alvarez S A. Quadratic-base computation of Four-impulse optimal rendezvous near circular orbit. J Guid Control Dyn, 2000, 23(1): 109–117
10 Prussing J E. Optimal impulsive linear systems: Sufficient conditions and maximum number of impulses. J Astron Sci, 1995, 43(2): 195–206
11 Carter T E, Hull D G. Optimal impulse space trajectories based on linear equations. J Optim Appl, 1991, 70(2): 277–297
12 Lawden D F. Fundamentals of space navigation. JBIS-J Br Interplanet Soc, 1954, 13(2): 87–101
13 Tschauner J. Elliptic orbit rendezvous. AIAA J, 1967, 5(6): 1110–1113
14 Yamanaka K, Ankersen F. New state transition matrix for relative motion on an arbitrary elliptical orbit. J Guid Control Dyn, 2002, 25(1): 60–66
15 Lawden D F. Time-closed optimal transfer by two impulses between coplanar elliptical orbits. J Guid Control Dyn, 1993, 16(3): 585– 587
16 Lawden D F. Optimal transfers between coplanar elliptical orbits. J Guid Control Dyn, 1994, 15(3): 788–791
17 Carter T E, Brient J, Hull D G. Linearized impulsive rendezvous problem. J Optim Theor Appl, 1995, 86(3): 553–584
18 Kim Y H, Spencer D B. Optimal spacecraft rendezvous using genetic algorithms. J Spacecr Rockets, 2002, 39(6): 859–865